Cloud Studies in Climate Research Programs with 8-Millimeter Wavelength Doppler Radar

R. A. Kropfli, S. Y. Matrosov, T. Uttal, and B. W. Orr
National Oceanic and Atmospheric Administration/Environmental Research Laboratories
Wave Propagation Laboratory
Boulder, CO 80303

Introduction

The National Oceanic and Atmospheric Administration's (NOAA) Wave Propagation Laboratory (WPL) operated a sensitive, 8-mm wavelength Doppler radar in three recent studies of clouds: the Cloud Lidar and Radar Exploratory Test (CLARET), the First ISCCP[a] Regional Experiment (FIRE II), and the Atlantic Stratocumulus Transition Experiment (ASTEX). Each experiment focused on cloud radiative and microphysical properties in order to improve cloud parameterizations in general circulation models. An overview of results from these experiments is presented to demonstrate the unique measurement capability of 8-mm wavelength (K_a-band) radar.

When integrated with other remote sensors such as a narrow-band infrared (IR) radiometer or a lidar, an mm-wavelength radar can greatly extend the quantitative microphysical information over that obtainable by any one of the sensors alone. Operating at 8 mm also has other distinct advantages for groundbased cloud remote sensing; such radars can penetrate optically thick and high liquid water content cloud layers. As a result, they can detect cirrus clouds above regions of light precipitation that attenuate lidar and shorter wavelength radar signals.

Radars at K_a-band are generally less sensitive to ground clutter than longer wavelength radars, making them operable at close range. Yet the wavelength is long enough to ensure that size parameters for cirrus cloud particles do not extend into the Mie scattering regime, greatly simplifying interpretation of the data. This paper illustrates the significant cloud observing capability of millimeter wavelength Doppler radar with recent examples from the WPL K_a-band Doppler radar (Kropfli et al. 1990).

(a) International Satellite Cloud Climatology Project.

Radar Capabilities

The WPL 8-mm wavelength radar was designed with good sensitivity and resolution to observe the small-scale structure and microphysical properties of clouds. During ASTEX, for example, it observed, with 37-m resolution, all marine boundary layer (MBL) stratus and stratocumulus clouds within 5 km of the radar. More dense nonprecipitating clouds and very light drizzle were routinely observed to ranges exceeding 35 km. Characteristics of the radar are summarized in Table 1.

A new offset Cassegrain antenna with good polarization performance is now being developed for this radar to study ice crystal shapes in cirrus clouds. Its capability for dual-polarization at circular, linear, and elliptical polarization basis states and the microphysical information obtainable from such measurements are described by Matrosov (1991) and by Matrosov and Kropfli (1993). These polarization states are made possible by a rotatable quarter-wave plate. This relatively unexplored technology based on Gaussian optics theory (Goldsmith 1991) may be

Table 1. Characteristics of WPL K_a-band radar.

Wavelength (cm)	0.866
Peak power (kW)	100
Pulse width (m)	37
Beam width (deg)	0.5
Dual polarization	yes
Scannable	yes
Transportable	yes
Doppler accuracy (4 s dwell)	<5 cm s^{-1}

appropriate for other millimeter wavelength radars now being developed for cloud research.

Ice Particle Size and Concentration

For cirrus clouds that are semitransparent in the IR, Matrosov et a!. (1992) suggested a method for estimating median ice particle size and concentration averaged vertically through the cloud. To do this, they invoked a two-stream radiation model and assumed a first-order gamma distribution of particle sizes. They showed that cirrus cloud optical thickness, t, can be estimated with an IR radiometer sensitive in the 9.9511.43 pm range, and that t varies as the fourth power of the median particle size, D_m. Also, radar reflectivity, Z, is shown to vary with the sixth power of D_m. Thus, D_m, along with the second parameter of the gamma distribution, N_o, is obtainable from these two relationships.

Recently, a technique for estimating ice particle fallspeed from zenith-pointing Doppler radar (Orr and Kropfli 1993) was incorporated into this two-sensor method to provide profiles of median particle size and concentration rather than vertically integrated estimates only (Matrosov et al. 1993). The additional relationship needed to achieve this is the power law dependency of fallspeed on particle diameter (Pruppacher and Klett 1978). An example of a profile of D_m obtained in this way from FIRE II data is shown in Figure 1.

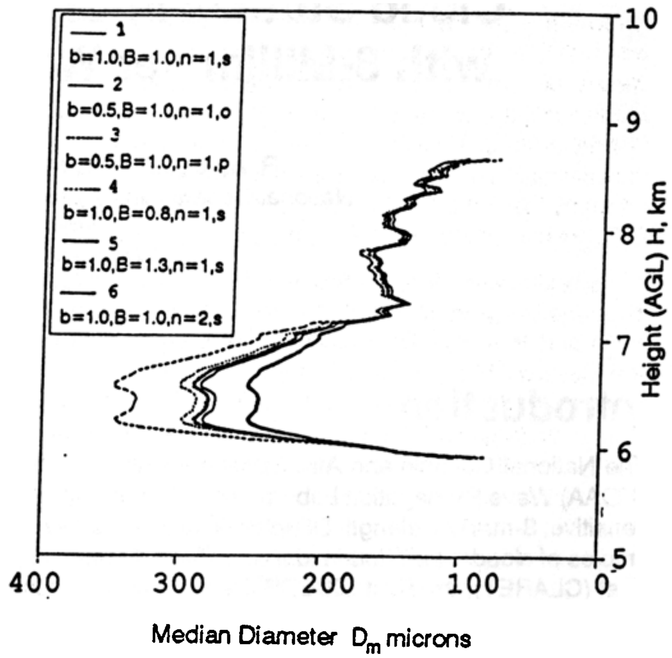

Figure 1. A profile of D_m obtained from radar reflectivity and Doppler velocity data along with an IR radiometer for a cloud observed on 26 November 1991 during FIRE II (Uttal et al. 1993). Curves are computed for different values of the particle aspect ratio, b, exponent in the fall velocity-size relationship, B, and order of the gamma distribution, n_o. The letters s, o, and p refer to whether particles are spherical, oblate, or prolate.

Ice Mass Path (IMP) and Ice Mass Flux (IMF)

Sassen (1987) showed that radar reflectivity can be used to provide an estimate of ice mass content (IMC) in cirrus clouds by means of an empirical power law relationship

$$IMC = 0.037Z_i0.696$$

where Z_i is radar reflectivity for ice particles. The two-sensor method mentioned above is expected to produce better results, however, because it accounts for independent particle size and concentration variations; includes inherently more measurement information; and has a physical basis for its validity. Its limitations are that it can be used only for cirrus clouds that are semitransparent in the IR, i.e., for optical depths less than about 2.5; and it produces only a pair of values (D_m and N_o) representing an average through the cloud depth. The method also cannot be used when liquid water is present. The radar-only method provides ice mass content versus height and is not limited by the cloud optical thickness or amount of cloud liquid present.

Despite the simple empirical approach, the reflectivity-only method for determining IMP (vertically integrated IMC) produces a result that is well-correlated with downwelling brightness temperature, T_b, at the surface. It therefore represents a cloud parameter that strongly influences downwelling IR radiation. Figure 2, from Uttal et al. (1993), shows the relationship between T_b measured with a PRT-5 IR radiometer and IMP computed from reflectivity when a horizontally homogeneous cirrus cloud with nearly constant base and top heights persisted for about 2.5 h. Also shown on this figure are curves of T_b versus IMP computed with a two-stream radiation transfer model for three values of D_m as shown by Matrosov et al. (1992). For the fixed D_m values indicated in the figure, the concentration of ice particles was allowed to vary to produce the variable IMP along the abscissa in Figure 2. A D_m value of 170 µm fits these data quite well.

Rough estimates of the vertical flux of ice mass were made by taking the product of the Doppler velocity and the IMC estimated from the Sassen IMC-reflectivity relationship. Averages of this product were obtained for five 25-min periods on 26 November 1991 during FIRE II. Although there were large variations in the five profiles (not shown), they seemed to have a similar characteristic shape, suggesting that an appropriate normalization might collapse the IMC profiles to a "universal" curve. Figure 3 shows the result of scaling height to the fraction of the distance from cloud base to cloud top and the IMF to the maximum flux value. Such normalization removed much of the profile-to-profile variability.

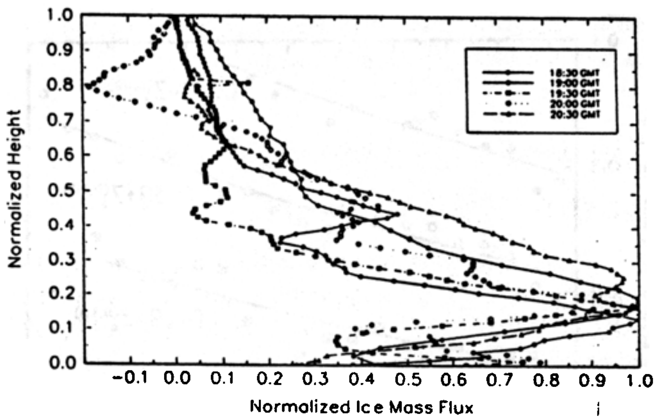

Figure 3. Profiles of IMF with the vertical scale normalized to cloud base and top and IMF normalized to the profile maximum for data obtained on 26 November 1991.

Hydrometeor Fallspeeds

A new approach has been taken to investigate relationships between reflectivity and the reflectivity-weighted ice particle fallspeed. This approach (Orr and Kropfli 1993) was demonstrated with data from the 8-mm radar during FIRE II. Doppler velocities were measured with an uncertainty of less than about 5 cm s^{-1} (Kropfli et al. 1990), and Doppler velocity profiles were obtained over 3-s intervals when the antenna was fixed in the vertical for many hours. Such Doppler velocity profiles represent the reflectivity-weighted particle fallspeed plus vertical air motion.

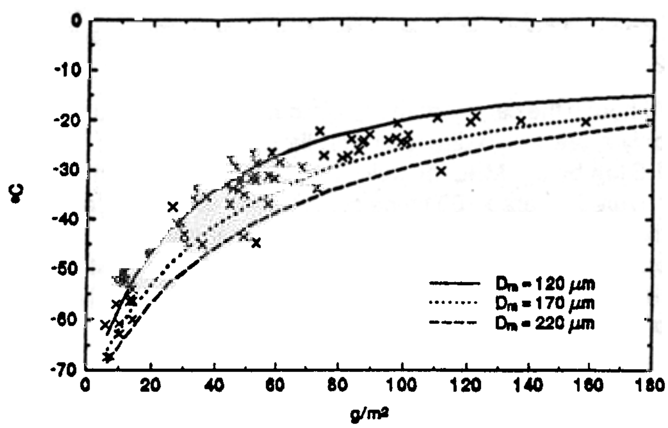

Figure 2. T_b versus IMP for a 2.5-h period on 4 October 1989. T_b was determined from a PRT-5 IR radiometer and IMP was computed from a vertical integration of IMC (Uttal et al. 1993).

The vertical air motion in cirrus clouds, when averaged over an hour or longer, is assumed to be small compared with typical ice particle fallspeeds. Thus, a long average of Doppler velocities closely approximates reflectivity-weighted particle fallspeeds; the averaged air motion contribution is negligible compared with typical particle fallspeeds of about 0.1 to 1 m s^{-1}.

Such averages were performed over 3 h for reflectivity intervals 1 dB wide, and the resulting averaged Doppler velocities were plotted against their corresponding reflectivity values (see Figure 4). The figure shows four relationships for different 560-m height intervals on 25 November 1991 during FIRE II. Shown on the figure are the central heights of each interval and the corresponding mean temperatures. The standard deviations of data about the best-fit curves are less than 4 cm s^{-1}, the trend of fallspeed increasing with reflectivity is clear, and the range of fallspeeds is consistent with expectations for cirrus cloud ice particles (Pruppacher and Klett 1978).

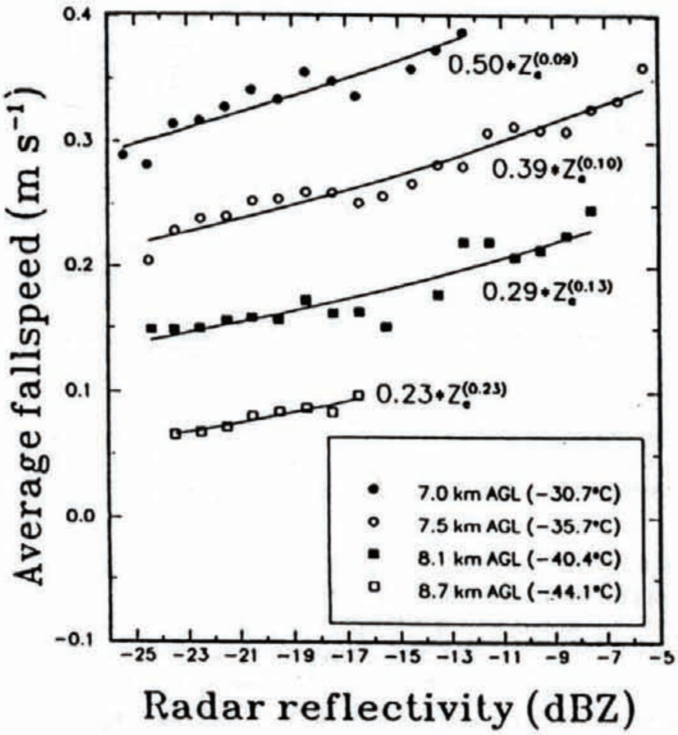

Figure 4. Fallspeed versus radar reflectivity observed during FIRE II on 25 November 1991.

Cloud Structure

The 8-mm wavelength radar, with its 37-m range resolution and 0.5° beam width, is able to document detailed spatial structure of clouds. Small-scale waves having amplitudes from 0.1 to 1 m s^{-1} and periods of 1 or 2 min ($\lambda \sim 2$ km), imbedded generating cells and fallstreaks, and multiple cloud layers were often observed in cirrus clouds during FIRE II. Figure 5 shows an example of a 6-km-deep cloud layer with precipitation streamers from cloud base at 2 km for data obtained on 21 November 1991 during FIRE II. Other examples of multiple cloud layers observed with this radar are found in Martner and Kropfli (1993).

Another notable example observed during ASTEX is that of the "microcell," a long-lived, small-scale cell having a weak reflectivity core (about 10 dBZ), a diameter less than 2 km, and a distinct vertically stacked convergence-divergence couplet (Kropfli and Orr 1993).

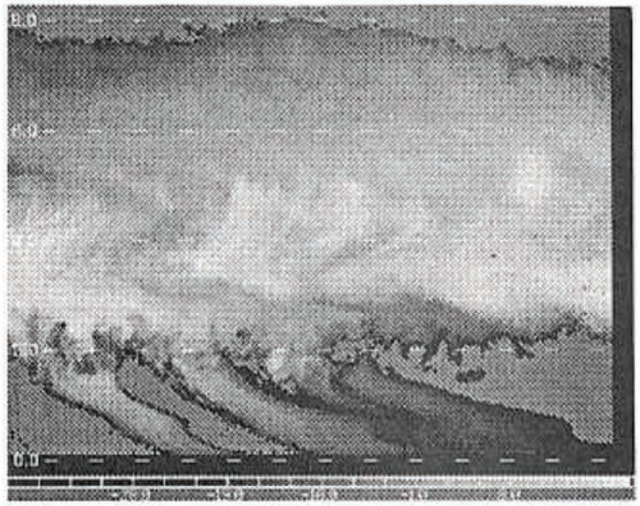

Figure 5. A 6-km-deep cloud with precipitation streamers.

Doppler velocity data from one elevation scan were interpolated to a 2-D Cartesian grid to generate an approximate visualization of the 2-D wind pattern in a microcell. The velocity measurements at the low elevation angles encountered in these observations were assumed to be reasonably good approximations to the horizontal wind projected onto the plane of the scan. Horizontal gradients of the interpolated values were used as estimates of divergence in the plane; the cross-plane contribution was not included. Finally, an upward integration was performed from the surface with a lower boundary condition of 0 m s^{-1} for the surface vertical air motion. The resulting 2-D wind field is shown in Figure 6.

Although the central core of a typical microcell was usually only a few km in diameter and limited vertically at about 1.5 km by the MBL inversion, the associated cloud often covered an area 100 times greater than the core. Despite the small size of the core region in which the cloudy air was apparently being generated and the weak reflectivities of the cores, these cells had unexpectedly long lifetimes, often exceeding 2 h.

Conclusions

We have outlined radar-based methods to estimate various cloud properties from the ground. These methods are

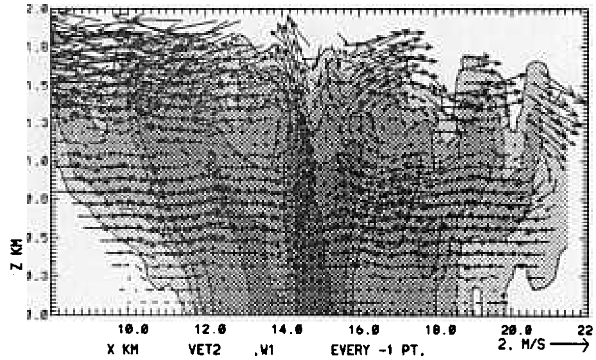

Figure 6. Two-dimensional wind field computed from an RHI scan through a microcell at 1142 Z on 21 June 1992. The arrow indicates a 5 m s^{-1} wind speed; the vertical axis is the height above the surface in km; and the horizontal axis represents the horizontal distance from the radar. Reflectivity contours are in 5 dB intervals with the highest contour at 10 dBZ.

theoretically plausible and show good consistency with other remote sensing measurements. Nevertheless, they are still in need of extensive validation with in situ and other remote sensing observations before they become routinely usable by the general scientific community.

Acknowledgments

Scott Shaver and Anne Keane contributed greatly to this work with their extensive help with the data processing. This research was funded in part by the U.S. Department of Energy's Atmospheric Radiation Measurement Program under contract 164514-A-91, and by the NOAA Climate and Global Change Program.

References

Goldsmith, P. F. 1991. Quasi-optics in radar systems. *Microwave J.* January, p. 79.

Kropfli, R. A., B. W. Bertram, and S. Y. Matrosov. 1990. The upgraded WPL dual-polarization 8-mm wavelength Doppler radar for microphysical and climate research. *Proc., 1990 Conference on Cloud Physics*, pp. 341-345. American Meteorological Society, Boston.

Kropfli, R. A., and B. W. Orr. 1993. Observations of microcells in the marine boundary layer with 8-mm wavelength Doppler radar. *Proc., 26th Conference on Radar Meteorology*, Norman, Oklahoma. American Meteorological Society, Boston.

Martner, B. E., and R. A. Kropfli. 1993. Observations of multi-layered clouds using K-band radar. *Proc., 31st Aerospace Sciences Meeting and Exhibit*, Reno, Nevada, AIAA-93-394, American Institute of Aeronautics and Astronautics, Washington, D.C.

Matrosov, S. Y. 1991. Prospects for the measurements of ice cloud particle shape and orientation with elliptically polarized radar signals. *Radio Sci.* **26**:847-856.

Matrosov, S. Y., and R. A. Kropfli. 1993. Cirrus cloud studies with elliptically polarized K_a-band radar signals: A suggested approach. *J. Ocean. Atmos. Techn.* (submitted).

Matrosov, S. Y., T. Uttal, J. B. Snider, and R. A. Kropfli. 1992. Estimation of ice cloud parameters from groundbased infrared radiometer and radar measurements. *J. Geophys. Res.* **97**:11567-11574.

Matrosov, S. Y., R. A. Kropfli, B. W. Orr, and J. B. Snider. 1993. Retrieval of vertical profiles of cirrus cloud microstructure parameters from Doppler radar and IR radiometer measurements. *J. Atmos. Sci.* (submitted).

Orr, B. W., and R. A. Kropfli. 1993. Estimation of cirrus cloud particle fallspeeds from vertically pointing Doppler radar. *Proc., 26th Conference on Radar Meteorology*, Norman, Oklahoma. American Meteorological Society, Boston.

Pruppacher, H. R., and J. D. Klett. 1978. *Microphysics of Clouds and Precipitation.* Reidel Publishing, Dordrecht, Holland.

Sassen, K. 1987. Ice cloud content from radar reflectivity. *J. Clim. Appl. Meteorol.* **26**:1050-1053.

Uttal, T., S. Y. Matrosov, J. B. Snider, and R. A. Kropfli. 1993. Relationships between ice water path and downward long wave radiation for clouds optically thin in the infrared: Observations and model calculations. *J. Appl. Meteorol.* (submitted).